Optical and Redox Properties of a Series of 3,4-Ethylenedioxythiophene Oligomers

Joke J. Apperloo,[a] L. "Bert" Groenendaal,[b] Hilde Verheyen,[b] Manickam Jayakannan,[a] René A. J. Janssen,*[a] Ahmed Dkhissi,[c] David Beljonne,[c] Roberto Lazzaroni,[c] and Jean-Luc Brédas[c, d]

Abstract: The optical and redox properties of a series of 3,4-ethylenedioxythiophene oligomers (EDOT*n*, $n = 1-4$) and their β,β'-unsubstituted analogues (T*n*, $n = 1-4$) are described. Both series are end capped with phenyl groups to prevent irreversible α-coupling reactions during oxidative doping. Absorption and fluorescence spectra of both series reveal a significantly higher degree of intrachain conformational order in the EDOT*n* oligomers. Oxidation potentials (E_{PA1} and E_{PA2}) determined by cyclic voltammetry reveal that those of EDOT*n* are significantly lower than the corresponding T*n* oligomers as a consequence of the electron-donating 3,4-ethylenedioxy substitution. Linear fits of E_{PA1} and E_{PA2} versus the reciprocal number of double bonds reveal significantly steeper slopes for the EDOT*n* than for the T*n* oligomers. This could indicate a more effective conjugation for the EDOT*n* series, confirmed by the fact that coalescence of E_{PA1} and E_{PA2} is reached already at relatively short chain lengths (≈ 5 EDOT units) in contrast to the T*n* series (> 10 thiophene units). The stepwise chemical oxidation of the EDOT*n* and T*n* oligomers in solution was carried out to obtain radical cations and dications. The energies of the optical transitions of the radical cations and dications as determined by UV/Vis/NIR spectroscopy were similar for the two series. These spectroscopic observations are consistent with quantum-chemical calculations performed on the singly charged molecules. Cooling solutions containing **T2**$^{\bullet+}$, **T3**$^{\bullet+}$, **EDOT2**$^{\bullet+}$, and **EDOT3**$^{\bullet+}$ revealed the reversible formation of dimers, albeit with a somewhat different tendency, expressed in the values for the dimerization enthalpy.

Keywords: conducting materials · oligomers · pi interactions · radical ions · redox chemistry

Introduction

As a unique derivative of polythiophenes, poly(3,4-ethylenedioxythiophene) (PEDOT), has been extensively investigated during the past decade.[1] PEDOT possesses several advantageous properties as compared with unsubstituted polythiophene and other polythiophene derivatives: it combines a low oxidation potential and moderate band gap with environmental stability in the oxidized state.[2, 3] Also, by blocking the β positions of the ring, the formation of $\alpha-\beta$ linkages during polymerization is prevented, resulting in a more regiochemically defined material. In addition to a high conductivity (ca. 600 S cm^{-1}),[4] PEDOT was found to be highly transparent in thin, oxidized films.[2, 3] As a result PEDOT has found several industrial applications.[5] The incorporation of EDOT building blocks in new conjugated systems has resulted in improved electrochromic behavior,[6, 7] polymers with a small intrinsic band gap,[6a, 8] and extended tetrathiafulvalene analogues with enhanced π-donor ability.[9] In order to understand the unique PEDOT behavior on a molecular level, it is of interest to systematically study the redox properties of well-defined EDOT oligomeric model compounds as a function of chain length.[10] In contrast to other oligothiophene derivatives, EDOT-based oligomers have received much less attention, possibly as a result of the fact that oligo-EDOT derivatives are sensitive to oxidation and thus difficult to handle. Reynolds et al. first synthesized

[a] Prof. R. A. J. Janssen, Dr. J. J. Apperloo, Dr. M. Jayakannan
Laboratory for Macromolecular and Organic Chemistry
Eindhoven University of Technology
PO Box 513, 5600 MB Eindhoven (The Netherlands)
Fax: (+31) 40-2451036
E-mail: r.a.j.janssen@tue.nl.

[b] Dr. L. Groenendaal, H. Verheyen
AGFA-Gevaert N.V.
R&D Materials/Chemistry department
Septestraat 27, 2640 Mortsel (Belgium)

[c] Dr. A. Dkhissi, Dr. D. Beljonne, Dr. R. Lazzaroni, Prof. J.-L. Brédas
Laboratory for Chemistry of Novel Materials
Center for Research in Molecular Electronics and Photonics
University of Mons-Hainaut
Place du Parc 20, 7000 Mons (Belgium)

[d] Prof. J.-L. Brédas
Department of Chemistry
The University of Arizona, Tucson, AZ 85721-0041 (USA)

  0947-6539/02/0810-2384 $ 20.00+.50/0

2,2′-bis-EDOT[11] and 2,2′:5′,2″-tris-EDOT.[12] The same group also reported the synthesis of several co-oligomers based on EDOT.[13] Very recently, Hicks et al. synthesized a first series of α,ω-bi(mesitylthio)-oligo-EDOTs and studied their UV/Vis and cyclovoltammetric properties.[14]

Here, we describe the optical and redox properties of a series of phenyl-blocked oligo-EDOTs (Scheme 1, EDOT*n*, $n=1-4$) in relation to the corresponding β,β'-unsubstituted oligothiophenes (Scheme 1, T*n*, $n=1-4$). The phenyl end caps have been incorporated to prevent irreversible coupling

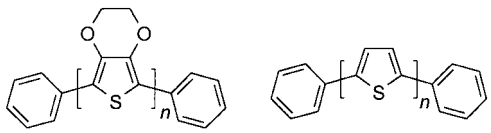

EDOT*n* (n = 1 - 4) T*n* (n = 1 - 4)

Scheme 1. Structure of the investigated phenyl-blocked oligo(3,4-ethylenedioxythiophene)s (EDOT*n*, $n=1-4$) and oligothiophenes (T*n*, $n=1-4$).

reactions during oxidation (doping), which are known to take place for oligothiophenes with less than six monomer units. Comparison of the absorption and fluorescence spectra in the two series reveals a significantly higher degree of intrachain conformational order in the EDOT*n* oligomers. For both series, the chemical and electrochemical formation of radical cations (first oxidation state) and dications (second oxidation state) was investigated. As a result of the stabilizing effect of the electron-donating ethylenedioxy substituents, the EDOT*n* oxidation potentials are significantly lowered compared with those of the β,β'-unsubstituted analogues and decrease more rapidly with increasing chain length. This implies a significantly higher conjugation between the monomer units for the EDOT*n* than for the T*n* oligomers. This is confirmed by the coalescence of the first and second oxidation potentials, which is observed at short chain lengths for EDOT*n*. On the other hand, the optical transitions observed in UV/Vis/NIR spectroscopy upon chemical doping of the EDOT*n* oligomers were similar to those of the T*n* oligomers, although some differences could be noted. These optical spectra were analyzed in the framework of a quantum-chemical description of the singly charged oligomers. The reversible formation of dimers upon cooling radical cation solutions of EDOT*n* oligomers has been established in detail, and the observations were compared with the behavior of T*n* oligomers. The optical signature associated with the dimerization has been explained in terms of interchain dimers and larger aggregates, consistent with the changes predicted from theoretical modeling based on an exciton approach.

Results and Discussion

Synthesis and characterization of EDOT*n* and T*n*: The α,ω-diphenyl-oligo(3,4-ethylenedioxythiophene)s (EDOT*n* $n=1-4$, Scheme 1) were synthesized as described in Scheme 2. By performing a combination of bromination/stannylation reactions and (a)symmetrical coupling reactions, the four phenyl-blocked oligomers were obtained in moderate to good

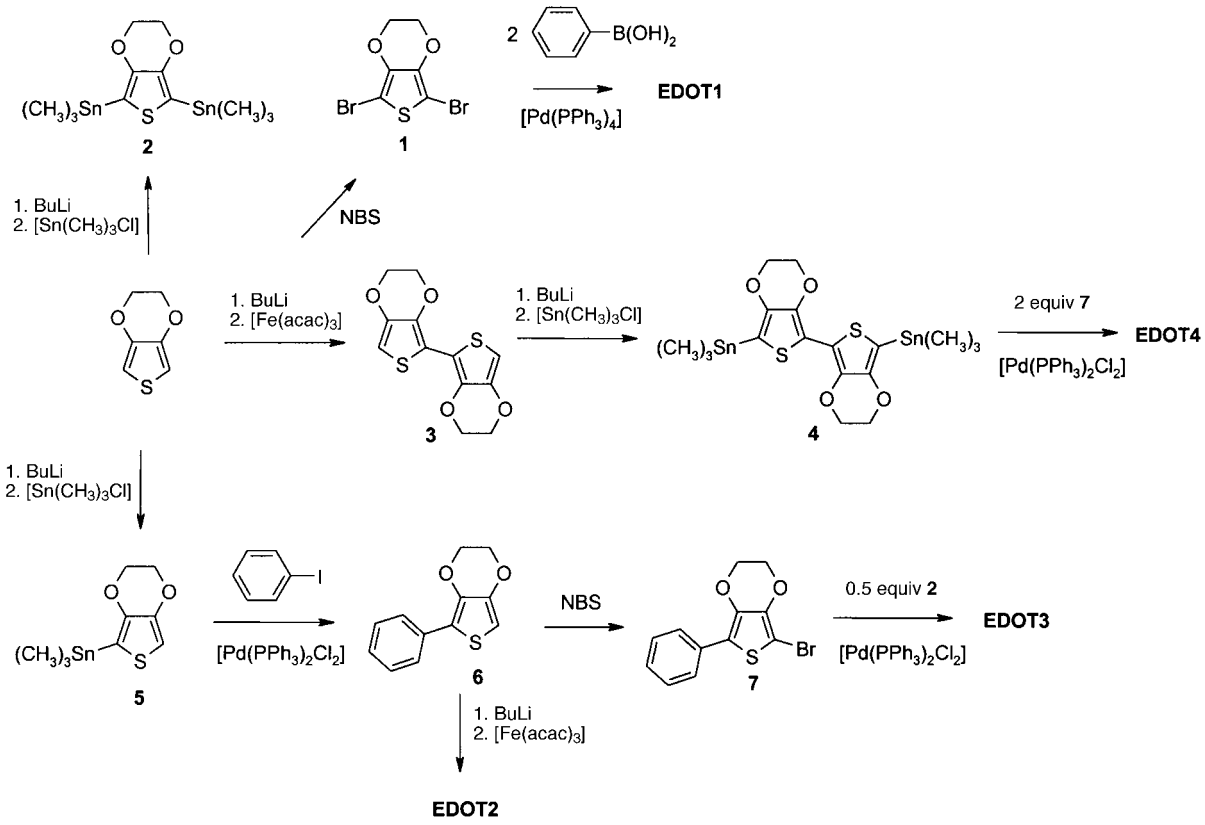

Scheme 2. Synthesis of EDOT*n* ($n=1-4$) oligomers.

  0947-6539/02/0810-2385 $ 20.00+.50/0

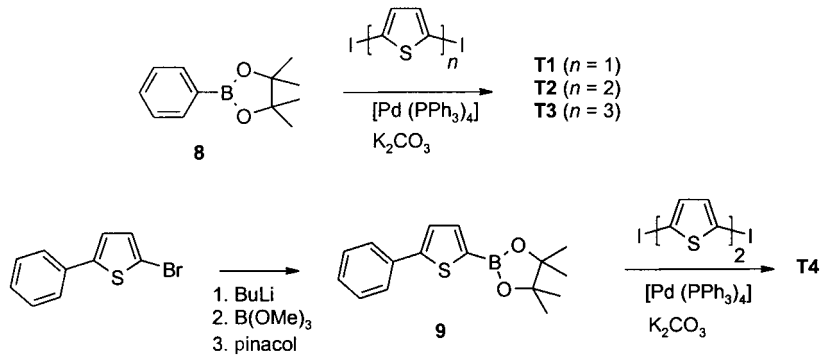

Scheme 3. Synthesis of T*n* ($n = 1-4$) oligomers.

yield. α,α'-Diphenyloligothiophenes (T*n*, $n = 1-4$) were synthesized in high purity by a palladium-catalyzed Suzuki coupling reaction of α,ω-diiodooligothiophenes with phenyl and 5-phenyl-2-thienyl boronic pinacol esters (Scheme 3). The structures of **EDOT1**–**EDOT3** and **T1**–**T3** were confirmed by ^{1}H and ^{13}C NMR spectroscopy, and the purity of the oligomers was found to be at least 99% by GC-MS analysis. The poor solubility of **EDOT4** and **T4** limits their complete structural characterization by NMR spectroscopy. However, MALDI-TOF-MS showed a single mass peak at $m/z =$ 482 amu corresponding to **T4**. The melting points of T*n* match the values reported in the literature.[15, 16] MALDI-TOF-MS analysis showed that **EDOT4** is only approximately 80% pure ($m/z = 714$). As contaminants **EDOT6** ($M = 994$) and **EDOT10** ($M = 1554$), resulting from organotin-bromo exchange followed by Stille couplings, can be analyzed. Although the **EDOT4** and **T4** samples were of lower purity, it was still possible to determine some of their characteristics. These are included in the following sections.

Absorption and fluorescence spectroscopy: Figure 1 shows the absorption (dashed lines) and emission (solid lines) spectra of EDOT*n* ($n = 1-4$), dissolved in dichloromethane. Despite the limited solubility of **EDOT3** and **EDOT4**, the spectral characteristics are concentration independent in the concentration ranges used, and this indicates that the molecules are not in an aggregated phase. The ethylenedioxy-substituted thiophene oligomers show a pronounced vibronic resolution in their absorption spectra in solution at room temperature, which becomes much more pronounced and shifts to lower energies upon cooling (not shown). The vibronic resolution seems to increase with oligomer chain length, and the noncontinuance of this trend in the case of **EDOT4** was attributed to the limited purity of the sample. In addition, the fluorescence spectra show an increasingly more pronounced 0–0 emission upon going to longer chain lengths, indicating an increase in the degree of intrachain conformational order. This has been attributed to S···O intramolecular interactions between the EDOT groups that result in planarization and rigidification of the conjugated system, and hence in an enhanced π-electron delocalization.[17]

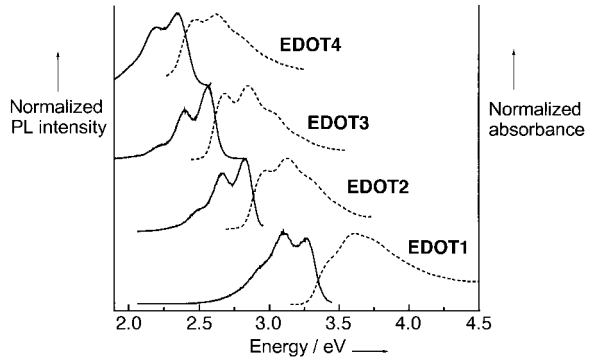

Figure 1. Normalized absorption (dashed lines) and emission (solid lines) spectra of EDOT*n* ($n = 1-4$), recorded in dichloromethane. The emission spectra are obtained by exciting at the maximum of the absorption spectrum. The spectra are offset vertically for clarity.

The absorption spectra of the corresponding T*n* oligomers (dashed lines, Figure 2), directly show the lack of vibronic resolution as compared with the EDOT*n* oligomers.[15, 16] The relatively broad, featureless transitions indicate a lower degree of conformational order (more specifically, the correspondence between ground and excited states' geometries is reduced). The emission spectra (solid lines) reveal a relatively less pronounced 0–0 vibronic transition compared with the EDOT*n* oligomers.

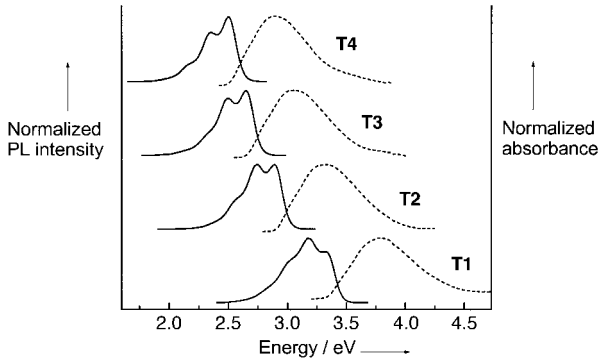

Figure 2. Normalized absorption (dashed lines) and emission (solid lines) spectra of T*n* ($n = 1-4$), recorded in dichloromethane. The emission spectra are obtained by exciting at the maximum of the absorption spectrum. The spectra are offset vertically for clarity.

Although the lack of vibronic resolution in the absorption spectra of T*n* makes an accurate determination difficult, it is evident that EDOT*n* oligomers have a significantly smaller Stokes' shift. The apparent increase in conformational order for the EDOT*n* oligomers might contribute to the lowering of the oxidation potential (see below) and, extrapolated to PEDOT, would favor an efficient intra- and interchain charge transport. We also note that the increased prominence of the emission 0–0 peak, with chain length in both series of oligomers, is indicative of a decreased relaxation energy in the excited state; a similar evolution has been observed earlier, for instance, in the case of oligophenylenevinylenes.[18]

  0947-6539/02/0810-2386 $ 20.00+.50/0 *Chem. Eur. J.* **2002**, *8*, No. 10

Cyclic voltammetry: For the EDOT*n* and T*n* oligomers the first oxidation wave, corresponding to the formation of the radical cation, was chemically reversible, and the anodic current was proportional to the square root of the scan rate as expected for a diffusion controlled electrochemical reaction. For **EDOT1** and **T1** the second oxidation wave is outside the electrochemical window of the electrolyte, although for **EDOT1** the onset of the second oxidation wave could be observed. The second oxidation wave for **EDOT2** and **EDOT3**, corresponding to dication formation, gave some indication of further reaction or conformational rearrangements in the reducing scan, although all forward scans were found to coincide. The voltammograms of **T2** and **T3** were reversible up to and including the second oxidation state. The solubility of **T4** was too low to perform cyclic voltammetry. The oxidation peak potentials, as determined for EDOT*n* and T*n* oligomers in dichloromethane (0.1M $TBAPF_6$), are collected in Table 1.

Table 1. Oxidation potentials E_{PA1} and E_{PA2} (in V versus SCE) determined in CH_2Cl_2 (electrolyte: 0.1M $TBAPF_6$).

	E_{PA1}	E_{PA2}
EDOT1	1.18	≈2
EDOT2	0.72	1.32
EDOT3	0.42	0.69
EDOT4	0.26[a]	0.39[a]
T1	1.42	>2
T2	1.14	1.65
T3	0.96	1.33

[a] Tentative values as the sample of **EDOT4** was not completely pure.

Comparison of the oxidation potentials of EDOT*n* and T*n* immediately shows the strong reduction of the oxidation potential as a result of the electron-rich substituent. Plotting the first and second oxidation potentials as a function of the reciprocal number of double bonds for EDOT*n* and T*n* (Figure 3) reveals a linear behavior. The slopes of these plots are significantly steeper for EDOT*n* than for T*n* (Figure 3). This suggests a significantly better conjugation for the EDOT*n* oligomers in comparison with their unsubstituted analogues, possibly as a result of their higher degree of intrachain order (see previous paragraph). For both systems, a coalescence of the first and second oxidation potentials is expected with increasing length of the system. This coalescence occurs at a lower number of double bonds for the EDOT*n* oligomers (≈**EDOT5**, according to the linear equations) than for the corresponding unsubstituted T*n* oligothiophenes (≈**T10**).

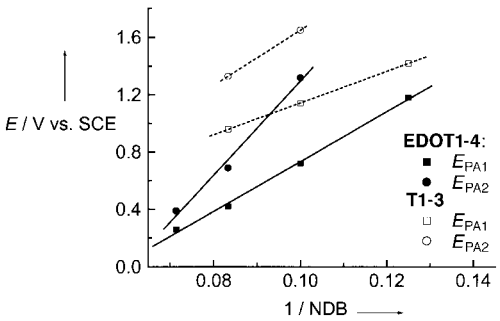

Figure 3. Evolution of E_{PA1} (squares) and E_{PA2} (circles) in dichloromethane (0.1M $TBAPF_6$) as a function of the reciprocal total number of double bonds (NDB) in the conjugated chain. The data for EDOT*n* ($n=1-4$) are depicted with closed symbols, the open symbols refer to T*n* ($n=1-3$).

Chemical oxidation to EDOT*n* radical cations: In Figure 4, the absorption spectra of the radical cations of EDOT*n* ($n=1-3$), obtained by stepwise addition of one equivalent of oxidizing agent to solutions in dichloromethane, are shown. In agreement with their increasing conjugation lengths, the radical cation transitions shift to lower energies going from **EDOT1** to **EDOT3**. In the case of **EDOT1**, reduction to the neutral state by addition of hydrazine, showed that further reaction occurred to some extent. In contrast, the oxidation of **EDOT2** and **EDOT3** to the singly oxidized state was found to be fully reversible.

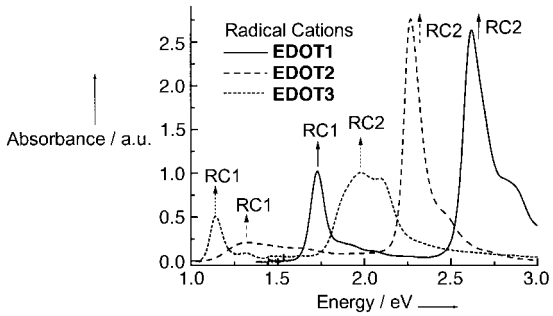

Figure 4. Absorption spectra of the radical cations (RC) of **EDOT1** (solid line), **EDOT2** (dashed line), and **EDOT3** (dotted line) in dichoromethane, obtained by adding one equivalent of oxidizing agent in a stepwise manner to their solutions. The spectra are normalized to the absorption of the neutral oligomers. The labels 1 and 2 refer to the low- and high-energy transitions, respectively.

A closer inspection of the appearance of the radical cation absorption bands reveals several differences for the three closely related compounds. The RC2 transition of **EDOT3** is quite broad, showing two equally intense maxima, and has a relatively low intensity. For **EDOT1** and **EDOT2**, the RC2 transitions are quite intense and rather narrow. While **EDOT1** shows a significantly intense RC1 transition, comparable to those generally observed for oligothiophenes, this transition has an almost negligible intensity for **EDOT2**. At present there is no explanation for these effects, but they could be related to specific conformational effects. Surprisingly, different absorption spectra were recorded for a solution containing singly oxidized **EDOT3** prepared by slow, stepwise addition of one equivalent of the oxidizing agent (solid line) or after fast addition (short dashed line, Figure 5). The latter slowly evolves in time into the solid line. This effect is found to be fully reproducible, but similar effects were not observed for **EDOT1** and **EDOT2**.

From the experiments described in the next paragraph, it was concluded that these time-dependent changes are not due to the slow dimerization of radical cations, since it was established that no more than 3% of the radical cations dimerized, even at 250 K. Furthermore, no concentration dependence was observed for this time-dependent effect. The

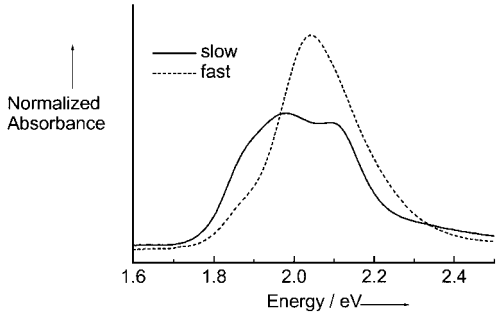

Figure 5. Absorption spectra for solutions containing singly oxidized **EDOT3** after slow, stepwise addition of one equivalent of the oxidizing agent (solid line), and after fast addition (dotted line) in dichloromethane.

slow nature of the process may point to a conformational change with a high energy of activation. A possible explanation could be a *syn*–*anti* isomerization, which presents a high activation energy once the molecules are in their oxidized state because of the significant quinoid character of the inter-ring bonds.

Chemical oxidation to T*n* radical cations: Figure 6 shows the absorption spectra of the radical cations of T*n* ($n=2-4$), obtained by adding one equivalent of oxidizing agent in a stepwise manner to their solutions. As a consequence of its high oxidation potential, the chemical oxidation of **T1** could not be realized. In contrast to the results for the EDOT*n* series, the intensities of the T$n^{\bullet+}$ transitions, relative to the neutral transition, increase with increasing length of the system.

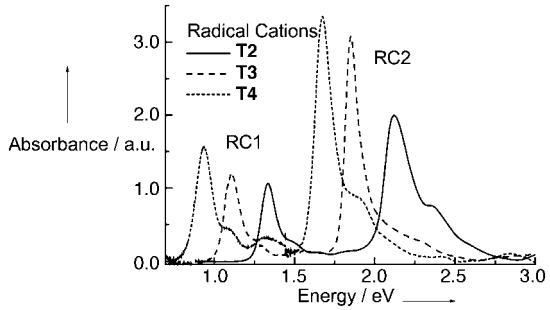

Figure 6. Absorption spectra of the radical cations (RC) of **T2** (solid line), **T3** (dashed line), and **T4** (dotted line) in dichloromethane, obtained by adding one equivalent of oxidizing agent in stepwise manner to their solutions. The spectra are normalized for unit neutral absorption. The labels 1 and 2 refer to the low- and high-energy transitions, respectively.

Chemical oxidation to EDOT*n* and T*n* dications: The formation of doubly oxidized EDOT*n* and T*n* oligomers by chemical oxidation was then investigated. The second oxidation potentials of **EDOT1**, **T1**, and **T2** are too high to obtain dications by chemical oxidation, even using a very strong oxidizing agent ($NOBF_4$). In the case of **EDOT2**, the radical cations could be partially converted into dications by using $NOBF_4$. However, strong side reactions occurred soon after the formation of **EDOT2**$^{2+}$, making its formation irreversible. The dication **EDOT3**$^{2+}$ can be formed reversibly, and a full interconversion of radical cations into dications can be observed. Similarly, the doubly oxidized states of T*n* could only be obtained in the cases of **T3** and **T4**.

Electronic transitions as a function of chain length: Table 2 shows the transition energies of the absorptions of all neutral (N) as well as singly (RC1 and RC2) and doubly (DC) oxidized states, determined for EDOT*n* and T*n*. From Figure 7, it can be seen that the energies of the transitions of neutral species and singly and doubly oxidized species of both the EDOT*n* ($n=1-4$, solid symbols and lines) and the T*n* ($n=1-4$, open symbols, dashed lines) series shift linearly with the reciprocal number of double bonds. For both series, all transitions shift with an approximately equal slope. It is clear that the absorption maxima of the charged species are very similar for the EDOT*n* series compared with the T*n* oligomers of equal chain length. As a consequence, by extrapolation of the absorption wavelengths of the dicationic species of both EDOT*n* and T*n* to values of *n* corresponding to longer chains, it can be expected that both PEDOT and PT (polythiophene) are transparent materials in their highly doped state, even at moderate backbone lengths.

Table 2. Summary of the absorption peak positions of neutrals (N), radical cations (RC), dications (DC), dimers (D), and stacked dimers (SD). Labels 1 and 2 refer to low and high energy, respectively. Data are given in eV.

	N	RC1	RC2	DC	D1	D2	SD
EDOT1	3.61	1.73	2.62				
EDOT2	3.13	1.32	2.27	1.96	1.50	2.47	≈2.75
EDOT3	2.85	1.15	1.93&2.10	1.68	1.31	2.11&2.26	≈2.52
EDOT4	2.63[a]	0.99[a]	1.7[a]	1.43[a]			
T1	3.79						
T2	3.32	1.33	2.12		1.63[31]	2.48&2.56[31]	
T3	3.05	1.11	1.85	1.59	1.41	2.19&2.30	
T4	2.88	0.94	1.67	1.37			

[a] Tentative values as the sample of **EDOT4** was not completely pure.

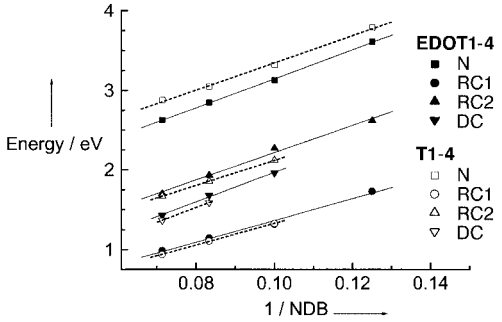

Figure 7. Evolution of the peak positions in the neutral (N, squares), radical cation (RC1, circles; RC2, upward triangles), and dication (DC, downward triangles) states observed in the UV/Vis/NIR spectra, as a function of the reciprocal number of double bonds along the conjugated chain. The data for the EDOT*n* ($n=1-4$) oligomers are depicted with closed symbols, the open symbols refer to the T*n* ($n=1-4$) oligomers. The data are summarized in Table 2.

ESR spectroscopy: For EDOT*n* ($n=1-3$), ESR spectra were recorded of solutions containing the corresponding radical cations. For **EDOT1**$^{\bullet+}$ and **EDOT2**$^{\bullet+}$, well-resolved ESR

0947-6539/02/0810-2388 $ 20.00+.50/0 *Chem. Eur. J.* **2002**, *8*, No. 10

spectra are obtained (Figure 8a and b). As a consequence of the increasing number of interacting nuclei, the degree of hyperfine splitting is larger for **EDOT2**$^{\bullet+}$ than for **EDOT1**$^{\bullet+}$. The spectrum of **EDOT3**$^{\bullet+}$ shows a single, featureless ESR transition without any resolved fine structure (Figure 8c). This is a result of the associated decrease of the average coupling

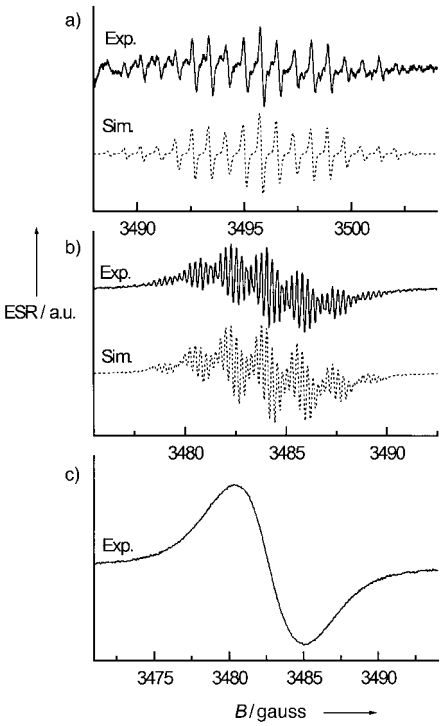

Figure 8. ESR spectrum (solid line) and simulation (dashed line) of **EDOT1**$^{\bullet+}$ (a), **EDOT2**$^{\bullet+}$ (b), and **EDOT3**$^{\bullet+}$ (c) in dichloromethane. Spectrum (a) was recorded at a frequency of 9.7971 GHz and the hyperfine coupling parameters used for the simulation are: $a(H) = 3.194$ gauss (2H), $a(H) = 2.362$ gauss (2H), $a(H) = 0.747$ gauss (4H), and $a(H) = 0.756$ gauss (2H) with a Lorentzian line shape and a 0.040 gauss line width. Spectrum (b) was recorded at 9.7626 GHz and the hyperfine coupling parameters used in the simulation are: $a(H) = 1.506$ gauss (4H), $a(H) = 1.770$ gauss (4H), $a(H) = 0.530$ gauss (4H), and $a(H) = 0.257$ gauss (2H) with a Lorentzian line shape and a 0.171 gauss line width. Spectrum (c) was recorded at a frequency of 9.7500 GHz.

constant as a consequence of the extended delocalization of the unpaired electron and the larger number of interacting nuclei. The spectra for **EDOT1** and **EDOT2** can be successfully simulated by using four different sets of hyperfine coupling constants in each case, corresponding to couplings to 10 and 14 protons, respectively (dashed lines, Figure 8a and b). The *g* values of 2.0023, 2.0022, and 2.0022, for **EDOT1**, **EDOT2**, and **EDOT3**, respectively, close to the free electron *g* value, are consistent with the formation of the EDOT*n* radical cations.

Dimerization of EDOT2$^{\bullet+}$ **and EDOT3**$^{\bullet+}$ **radical cations**: Monocation radicals of oligothiophenes,[19–22] oligopyrroles,[23] mixed thiophene–pyrrole oligomers,[24] oligo(*p*-phenylenevinylenes),[25] and oligo(thienylenevinylenes)[26, 27] form dimers in solution at high concentrations or low temperatures. These dimers are spinless and exhibit generally two strong optical absorptions. The structure of the dimers has been described as a face-to-face complex of the singly charged π-conjugated oligomers. In general the two optical transitions of the dimer are blue shifted with respect to those of the radical cation, which has been explained by a Davidov interaction between the transition dipole moments of the two radical cations in a face-to-face π dimer.[28] Two X-ray structures of oligomer radical cations support the geometrical structure of these π dimers in the solid state.[29, 30] The extent of dimerization in solution depends on a subtle balance between attractive and repulsive interactions, in which the solvent, the nature of the π-conjugated backbone, and the number and nature of backbone substituents (by the van der Waals interactions) play decisive roles.[31] As an alternative to π dimerization, σ dimers have been proposed.[32] Based on a detailed electrochemical study of diphenyloligoenes evidence has been provided that their radical cations form σ dimers rather than π dimers.[32] The formation of σ dimers from radical cations in solution has also been suggested for end-capped bithiophenes, bipyrroles, and related structures.[30, 33]

Using variable-temperature UV/Vis/NIR spectroscopy on solutions containing the EDOT*n* compounds in their singly oxidized state, the tendency to form dimers was investigated. Because of the lack of stability of the singly oxidized state of **EDOT1**, no dimerization experiments were performed with this compound or with the not completely pure **EDOT4**. For solutions containing **EDOT2**$^{\bullet+}$ and **EDOT3**$^{\bullet+}$, clear evidence of dimerization was observed upon cooling: a decrease of the intensity of the radical cation is accompanied by two new π-dimer transitions (D1 and D2) at higher energy. The blue shift of the D1 and D2 transitions with respect to RC1 and RC2 is consistent with the formation of π dimers for EDOT*n*$^{\bullet+}$.[28]

For **EDOT2**$^{\bullet+}$, cooling at a concentration of $\approx 5 \times 10^{-6}$ M in a 1 cm cell only showed some minor changes, starting at about 200 K. However, at a significantly higher concentration ($\approx 3.2 \times 10^{-5}$ M), the radical cations had already dimerized to some extent at room temperature, and the dimerization went to completion (i.e., complete loss of the RC1 and RC2 transitions) in the temperature range studied (cooling from 300 K down to 190 K, see Figure 9). Magnification of the low-energy area (left inset of Figure 9) clearly confirms two interconverting transitions upon cooling. The major spectral

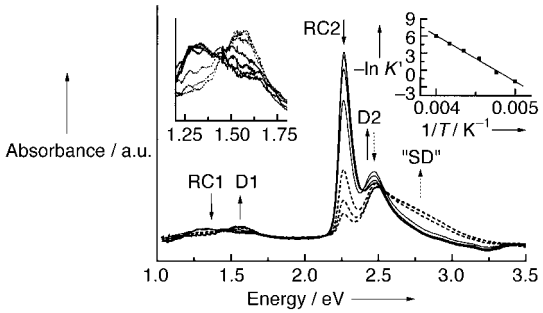

Figure 9. Absorption changes upon cooling a 3.2×10^{-5} M solution of **EDOT2**$^{\bullet+}$ in dichloromethane. The graph shows the reversible formation of π dimers (D1 and D2) from radical cations (RC1 and RC2) from 250–220 K (solid lines), and the subsequent formation of stacked dimers (SD) from π dimers from 210–190 K (dashed lines). The left top inset shows a magnification of the low-energy area. The right top inset shows a van't Hoff plot ($-\ln K'$ versus $1/T$, ($K' = K \times [A_T]$)).

changes only started at 250 K. This was quite surprising in view of the fact that dimers were already present at room temperature. Between 250 and 210 K an isosbestic point was observed at 2.39 eV, which is a clear indication of the interconversion of two species. At 210 K, the isosbestic point shifts to 2.51 eV. Apart from the dimerization process, new features appeared in the spectrum below 210 K: the transitions associated with the free radical cations continued to decrease, but at the same time, the intensity of the dimer transitions (more pronounced for D2) decreased, accompanied by an increase of new transitions at higher energy, especially in the RC2/D2 region. These phenomena had been observed previously for thienylenevinylene oligomers[27] and were attributed to stacking of π dimers (thus, their label SD (stacked dimer)), consistent with the additional blue shift.

Figure 10 shows the room-temperature spectra of the singly oxidized **EDOT2** in solutions at three different concentrations (5×10^{-6}, 3.2×10^{-5}, and 1.6×10^{-4} M), normalized to unit neutral absorbance (depicted by the dash-dotted line). After normalization, the neutral absorption spectra were identical

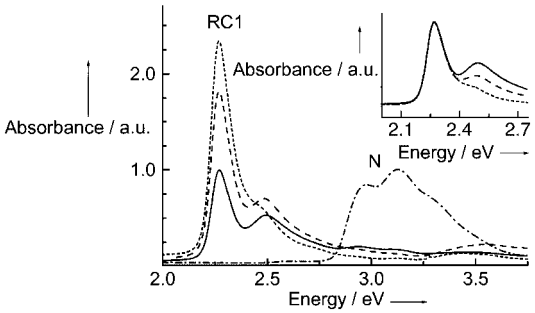

Figure 10. Absorption spectra for different concentrations of solutions in dichloromethane of singly oxidized **EDOT2**$^{\bullet+}$ (5×10^{-6} (dotted line), 3.2×10^{-5} (dashed line), and 1.6×10^{-4} M (solid line), normalized for unit neutral absorbance (depicted with the dash–dotted line)). The inset shows the same **EDOT2**$^{\bullet+}$ spectra normalized at 2.27 eV.

for all concentrations, and this indicated the molecularly dissolved nature of the neutral molecules. However, clear concentration dependence was observed in the absorption spectra of the singly oxidized molecules, consistent with the presence of a dimerization equilibrium. Cooling the most concentrated solution of **EDOT2**$^{\bullet+}$ gave rise to a large degree of precipitation, in addition to the further dimerization that took place.

Cooling solutions containing **EDOT3**$^{\bullet+}$ (Figure 11) clearly revealed the interconversion of radical cations into dimers in the low-energy region of the absorption spectrum (RC1 → D1), showing blue-shifted dimer transitions and an isosbestic point. The high-energy region was somewhat more complex. The new transition arising at higher energies (marked D2, Figure 11) clearly corresponded to dimer formation, but the transition marked with a double asterisk, seemed to possess contributions from free radical cations and from dimers, which obscured the identification of an isosbestic point. Calculations of the enthalpy of dimerization (see below) showed that, at 250 K in dichloromethane, 97% of singly oxidized **EDOT3**$^{\bullet+}$ was still present as free radical cations. At

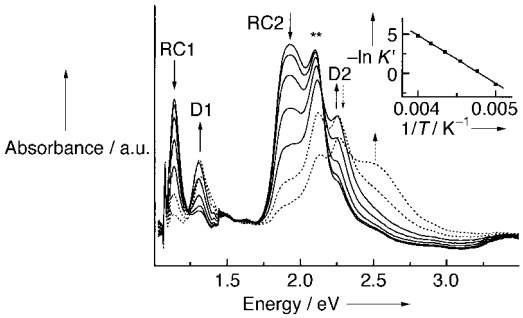

Figure 11. Absorption changes upon cooling a 5×10^{-6} M solution of **EDOT3**$^{\bullet+}$ in dichloromethane (250–210 K: solid lines; 200–190 K: dashed lines). The graph shows the reversible formation of π dimers (D1 and D2) and stacked dimers (SD) from radical cations (RC1 and RC2). The right top inset shows a van't Hoff plot ($-\ln K'$ versus $1/T$, ($K' = K \times [A_T]$)).

the lowest temperatures (210 down to 190 K), stacked π dimers (SD) as described for **EDOT2**$^{\bullet+}$, were also observed for **EDOT3**$^{\bullet+}$. The absorption maxima of dimers (D) and stacked dimers (SD) of **EDOT2**$^{\bullet+}$ and **EDOT3**$^{\bullet+}$ are collected in Table 2.

The spinless nature of the dimers formed upon cooling of **EDOT2**$^{\bullet+}$ and **EDOT3**$^{\bullet+}$ solutions was confirmed by ESR experiments. The ESR signal intensity of the radical cations decreased upon lowering the temperature. This process was reversible, indicating that no secondary processes such as degradation are involved.

Dimerization of T2$^{\bullet+}$ **and T3**$^{\bullet+}$ **radical cations**: Dimerization of **T2**$^{\bullet+}$ has been reported previously.[31] The D1 and D2 transition energies are given in Table 2. Cooling solutions containing **T3**$^{\bullet+}$ in dichloromethane revealed an almost complete dimerization from 250–190 K (Figure 12) with dimer transitions at 1.41 (D1) and 2.19/2.30 eV (D2). The spectra nicely showed isosbestic points at 1.18 and 2.08 eV. The overall spectra looked considerably different from those for **EDOT3**$^{\bullet+}$ (Figure 11). Especially the low-energy dimer transitions (D1) were found at significantly higher energies for T*n* compared with EDOT*n*, while the radical cation transitions from which they originated were quite similar (Table 2). Although the exact nature of the differences was not clear, they could be due to the conformational differences discussed above.

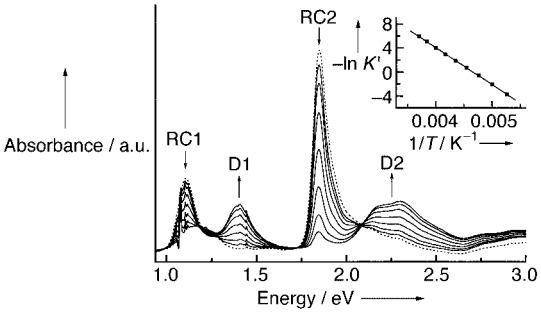

Figure 12. Absorption changes upon cooling a 5×10^{-6} M solution of **T3**$^{\bullet+}$ in dichloromethane (290 K (dashed line); 250–190 K (solid lines)). The graph shows the reversible formation of π dimers (D1 and D2) from radical cations (RC1 and RC2). The right top inset shows a van't Hoff plot ($-\ln K'$ versus $1/T$, ($K' = K \times [A_T]$)).

0947-6539/02/0810-2390 $ 20.00+.50/0 *Chem. Eur. J.* **2002**, *8*, No. 10

Energetics of dimerization: The EDOT$n^{\bullet+}$ enthalpy of dimerization ΔH_{dim} could be determined from the decrease of the RC1 and RC2 bands, or from the increase of the D1 and D2 bands, by plotting $-\ln K$ versus $1/T$ (van't Hoff plot, right top insets, Figure 9 and 11), where K is defined as $(1-x_M)/(2x_M^2[A_T])$ with x_M the fraction of monomeric monocation radicals, and $[A_T]$ the total concentration of singly oxidized species. The ΔH_{dim} values obtained on the basis of the decreasing RC2 transition were -60 ± 7 kJ mol^{-1} for **EDOT2**$^{\bullet+}$ and -50 ± 5 kJ mol^{-1} for **EDOT3**$^{\bullet+}$. The somewhat lower value for **EDOT3** contradicted the apparently higher tendency for **EDOT3**$^{\bullet+}$ to dimerize, which forms dimers at significantly lower concentrations than **EDOT2**. Moreover, it is in contrast to the generally observed more negative ΔH_{dim} values for longer systems.[19–27] This stresses the importance of entropic contributions to the dimerization process for the EDOTn oligomers. The ΔH_{dim} value for both **T2** and **T3** was -50 ± 5 kJ mol^{-1} (inset Figure 12, reference [31]).

Quantum-chemical calculations: As usually found in conjugated materials, switching from the neutral to the charged form of the phenyl-capped EDOT oligomers induces significant bond-length modifications leading to the appearance of a quinoid character on the aromatic rings.[34] These self-localized geometric deformations of the radical cation, corresponding to the formation of polaron defects,[35, 36] lead to a redistribution of the linear absorption cross section as a result of the formation of polaronic electronic levels within the HOMO–LUMO energy gap (see Figure 13). In the case of singly charged oligomers, two new optical transitions usually appear in the absorption spectrum, which correspond to excitations from the HOMO level to the lower lying polaronic P1 level and the transition from P1 to the higher lying polaronic P2 level.

In Table 3, we present a comparison between the measured and calculated (at both the AM1/FCI and INDO/SCI levels) excitation energies for the lowest two optical transitions, denoted RC1 and RC2, in **EDOT1**$^{\bullet+}$, **EDOT2**$^{\bullet+}$, and **EDOT3**$^{\bullet+}$; the corresponding oscillator strengths and CI (configuration interaction) expansion coefficients are also reported. Figure 14 shows the AM1/FCI simulated absorption spectra of the cationic species of phenyl-capped EDOT oligomers of increasing size. Excellent agreement is found between the spectroscopic and theoretical excitation energies, with deviations of the order 0.1–0.2 eV (except for **EDOT1**).

Table 3. Main parameters for the first, RC1, and second, RC2, optical transitions in the singly charged form of the phenyl-capped EDOTn oligomers (E^* denotes the excitation energy and O.S. the oscillator strength).

	Measured E^* [eV]	INDO/SCI E^* [eV] (O.S.)	AM1/FCI E^* [eV] (O.S.)	INDO/SCI wavefunction	AM1/FCI wavefunction
EDOT1					
RC1	1.73	1.60 (0.01)	1.37 (0.12)	-0.47[P1 → P2] $+0.82$[H → P1]	0.67[H → P1] -0.48[P1 → P2]
RC2	2.62	2.30 (0.41)	2.19 (0.72)	0.77[P1 → P2] $+0.34$[H → P1]	0.35[H → P1] $+0.77$[P1 → P2]
EDOT2					
RC1	1.32	1.44 (0.007)	1.32 (0.11)	-0.68[P1 → P2] $+0.55$[H → P1]	0.76[H → P1] -0.52[P1 → P2]
RC2	2.27	2.23 (1.03)	2.03 (1.00)	0.62[P1 → P2] $+0.66$[H → P1]	0.47[H → P1] $+0.72$[P1 → P2]
EDOT3					
RC1	1.15	1.20 (0.008)	1.05 (0.11)	-0.69[P1 → P2] $+0.58$[H → P1]	0.66[H → P1] -0.43[P1 → P2]
RC2	1.93&2.10	2.04 (1.33)	1.97 (1.21)	0.62[P1 → P2] $+0.64$[H → P1]	0.47[H → P1] $+0.75$[P1 → P2]

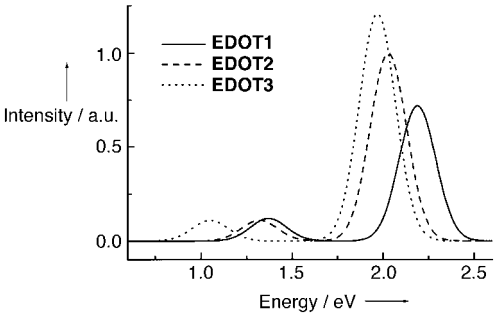

Figure 14. AM1/FCI simulated optical absorption spectra of the singly charged phenyl-capped EDOTn oligomers.

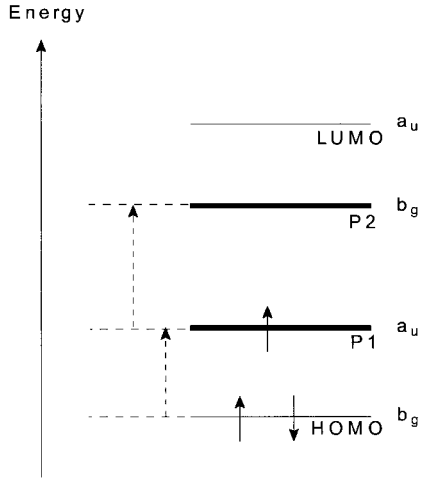

Figure 13. Schematic energy diagram of a positive polaron in a conjugated chain with C_{2h} symmetry. The polaronic levels are shown by bold lines; the two lowest dipole-allowed electronic excitations are shown by dashed arrows.

As expected, the excited states giving rise to the lowest two absorption bands are described by the combination of electronic excitations involving the HOMO, LUMO, and P1 and P2 polaronic levels. However, in contrast to the situation encountered in phenylenevinylene oligomers, for which RC1 and RC2 correspond mainly to the HOMO → P1 and P1 → P2 transitions, respectively,[37] the lowest two excited states in the thiophene-based molecules involve a pronounced mixing between these two electronic configurations (see Table 3). We explain this difference by the more rigid character of the conjugated skeleton in phenylene-based materials, which prevents large lattice distortions upon removal of one electron; smaller geometric deformations then translate into shallower drifts of the polaronic levels inside the gap, which leads to well-separated HOMO → P1 and P1 → P2 excitations

and the appearance of two intense bands on the optical spectrum of the charged species.

In the T*n* and EDOT*n* oligomers investigated here, owing to the more pronounced lattice deformations, the HOMO → P1 and P1 → P2 excitations are closer in energy (the polaronic levels are shifted deeper into the band gap), and significant mixing between these configurations occurs that results in a shift of oscillator strength from RC1 to RC2. As a matter of fact, while the lowest excited state corresponds essentially to an antisymmetric, that is, destructive combination of the HOMO → P1 and P1 → P2 excitations, the second one results from a symmetric, that is, constructive mixing of the same configurations. This highlights the need for a proper handling of electron correlation effects and rationalizes the weaker absorption intensity calculated for RC1. Note that this effect is particularly pronounced at the INDO/SCI level, at which the lowest excited state carries a vanishingly small oscillator strength (spectra not shown). The distribution of oscillator strength between the lowest two excited states predicted by the calculations is consistent with the experimental results and indicates a much stronger absorbance in the region of the RC2 transition with respect to RC1 (particularly for **EDOT2**$^{\bullet+}$).

The experimental absorption spectra of **EDOT2**$^{\bullet+}$ and **EDOT3**$^{\bullet+}$ reveal the emergence of new transitions upon cooling the solutions, which are associated with the formation of π dimers and stacked dimers. These excitations result from exciton coupling between excitations on adjacent conjugated chains and can be modeled accurately in the framework of an exciton model, wherein long-range Coulomb interactions are treated on the basis of an atomic expansion of the transition moment in the isolated chain.[38] Since the conjugated chains are likely to pack with their main axis parallel, interchain interactions lead to a blue shift of the optical transition with respect to the isolated chain by an amount corresponding to approximately half the exciton splitting.[38] By considering cofacial arrangements of two conjugated chains and an interchain separation of 4 Å, we have estimated at the INDO-SCI level the blue shift to be approximately 0.15–0.2 eV for the RC2 transition in the series **EDOT1**, **EDOT2**, and **EDOT3**. This compares very well with the experimental energy difference measured between RC2 and D2 in these molecules, of the order 0.2 eV. However, the same calculations predict a vanishingly small exciton coupling (less than 0.1 eV) for the lowest RC1 transition (this was expected from the low oscillator strength of this excitation), which is not consistent with the experimental observation (indicating a shift from RC1 to D1 of the same order of magnitude, albeit slightly smaller than that from RC2 to D2, i.e., ≈0.15 eV). This discrepancy certainly warrants further investigations, which are now in progress. Finally, we note that, for an infinite one-dimensional stack of interacting oligomers, the exciton coupling should be twice the value calculated for the dimer when retaining only nearest neighbor interactions. Comparison between the location of the RC2, D2, and SD transitions, as measured experimentally (Table 2), indicates that this holds true to a large extent. This suggests the formation of large aggregates in solution at low temperature.

In order to gauge the influence of the electron-donating 3,4-ethylenedioxy substitution on the optical properties of the EDOT*n*$^{\bullet+}$ series, we have also modeled the absorption spectra of the corresponding phenyl-capped unsubstituted oligothiophenes by using the same methodology (INDO/SCI and AM1/FCI excited-state calculations on the basis of ab initio/6-31G optimized geometries). The AM1/FCI simulated optical spectra are shown in Figure 15, and the position and oscillator strength of the lowest two transitions compared with the experimental data in Table 4. As found experimentally, the relative intensities and locations of the two main absorption bands as calculated in EDOT*n*$^{\bullet+}$ and T*n*$^{\bullet+}$ oligomers of equivalent sizes are very similar. In addition, the same description of the lowest two excited states as that discussed for the EDOT*n* molecules prevails. Thus, the electron-donating ethylenedioxy bridges appear to contribute only weakly to the excitations of the singly charged systems, while they clearly influence the optical transitions of the neutral systems (this results in a red shift of the first absorption peak when going from T*n* to EDOT*n*, which is estimated to be of the order of 0.2 eV from the experimental data in dichloromethane; similar shifts are predicted from calculations on the neutral oligomers).[39] In spite of the very similar shape of the absorption spectra of the singly charged EDOT*n* and T*n* oligomers at room temperature, the new transitions assigned to dimers in cooled solutions are blue shifted with respect to

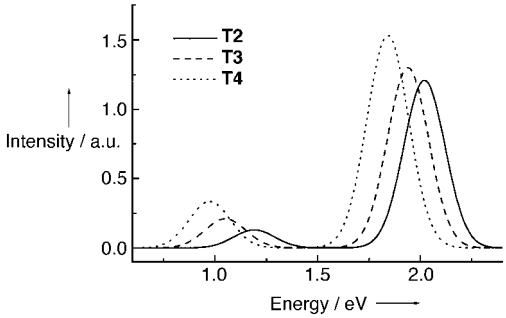

Figure 15. AM1/FCI simulated optical absorption spectra of the singly charged phenyl-capped T*n* oligomers.

Table 4. Main parameters for the first, RC1, and second, RC2, optical transitions in the singly charged form of the phenyl-capped T*n* oligomers (*E** denotes the excitation energy and O.S. the oscillator strength).

	Measured *E** [eV]	INDO/SCI *E** [eV] O.S.	AM1/FCI *E** [eV] O.S.	INDO/SCI wavefunction	AM1/FCI wavefunction
T2					
RC1	1.33	1.43 (0.002)	1.19 (0.13)	0.77[P1 → P2] − 0.53[H → P1]	−0.78[H → P1] +0.49[P1 → P2]
RC2	2.12	2.24 (1.24)	2.02 (1.21)	0.52[P1 → P2] +0.73[H → P1]	0.48[H → P1] +0.76[P1 → P2]
T3					
RC1	1.11	1.15 (0.001)	1.05 (0.21)	0.71[P1 → P2] − 0.54[H → P1]	−0.79[H → P1] +0.45[P1 → P2]
RC2	1.85	1.95 (1.38)	1.94 (1.30)	0.57[P1 → P2] +0.66[H → P1]	0.43[H → P1] +0.79[P1 → P2]
T4					
RC1	0.94	1.07 (0.01)	0.97 (0.34)	−0.66[P1 → P2] +0.58[H → P1]	−0.81[H → P1] +0.40[P1 → P2]
RC2	1.67	1.82 (1.58)	1.85 (1.03)	0.61[P1 → P2] +0.62[H → P1]	0.33[H → P1] +0.74[P1 → P2]

RC1 and RC2, to a larger extent in T*n* (≈0.3–0.4 eV) than in EDOT*n* (≈0.2 eV). Since the single-chain electronic excitations in the cationic forms of EDOT*n* and T*n* have a similar nature, the difference in exciton splitting measured for the two series of molecules is likely to originate in a different packing of the conjugated chains, with closer contacts (stronger interactions) in the case of the oligothiophenes (since these show the largest exciton couplings). To confirm this hypothesis, calculations are in progress to model the interchain interactions in EDOT*n* and T*n* oligomers.[39]

Conclusion

The optical and redox properties of 3,4-ethylenedioxythiophene oligomers (EDOT*n*, $n=1-4$) and their β,β'-unsubstituted analogues (T*n*, $n=1-4$) have been studied. Both series were doubly end capped with phenyl groups to prevent irreversible coupling reactions during doping. The absorption and fluorescence spectra of neutral EDOT*n* oligomers showed a much more resolved vibronic structure and smaller Stokes' shifts than the T*n* oligomers. This indicated a high degree of intrachain conformational order in the EDOT*n* compounds. Cyclic voltammetry revealed that the EDOT*n* oxidation potentials were significantly lower than those of the β,β'-unsubstituted T*n* oligomers as a result of the electron-releasing effect of the ethylenedioxy substituent. More surprisingly, a linear fit of the oxidation potentials, as a function of the reciprocal number of double bonds, revealed a much steeper slope for the EDOT*n* oligomers than for their unsubstituted analogues. This indicated that the EDOT*n* oligomers possessed a significantly higher conjugation than the corresponding T*n* oligomers, possibly due to the higher degree of intrachain order that could be inferred from their absorption and fluorescence spectra. Furthermore, coalescence of the first and second oxidation potentials was achieved much faster for the EDOT*n* than for the T*n* series. The stepwise chemical oxidation of the EDOT*n* and T*n* oligomers in solution was accomplished up to the dicationic state (if their oxidation potentials were sufficiently low). The observations were similar for the two series. Cooling solutions containing **T2**$^{\bullet+}$, **T3**$^{\bullet+}$, **EDOT2**$^{\bullet+}$, and **EDOT3**$^{\bullet+}$ revealed the reversible formation of dimers, albeit with a somewhat different tendency, expressed in the values determined for the enthalpy of dimerization.

Comparison of the results of the homologous EDOT*n* and T*n* series revealed that the exceptional properties of PEDOT as a colorless, transparent, and highly conducting polymer in the oxidized state, are a consequence of the low oxidation potential due to the electron-releasing ethylenedioxy substituent. Although the neutral state of the EDOT*n* oligomers possesses a higher degree of conformational order than the T*n* molecules, the absorption spectra in the first and second oxidized states were remarkably similar for the two series. This was consistent with the fact that highly oxidized states of simple poly(3-alkylthiophenes) could be rendered transparent and colorless in the visible region, although they lack the stability of PEDOT under ambient conditions.[40] In addition, correlated quantum-chemical calculations performed on the singly charged species confirm the similarity between the electronic excitations in EDOT*n* and T*n* oligomers and provide excitation energies in excellent agreement with experiments. The appearance of new transitions in the π dimers to the blue of the isolated chain optical bands can be accounted for by an exciton model describing interactions between neighboring charged molecules.

Experimental Section

General: Commercial grade solvents were purified, dried, and deoxygenated following standard methods. Cyclic voltammograms were recorded in CH_2Cl_2 or CH_3CN with 0.1 M tetrabutylammonium hexafluorophosphate ($TBAPF_6$) as the supporting electrolyte by using a Potentioscan Wenking-POS73 potentiostat. The working electrode was a platinum disc (0.2 cm^2), the counter electrode was a platinum plate (0.5 cm^2), and a saturated calomel electrode was used as the reference electrode, calibrated against a Fc/Fc^+ couple (+0.470 V vs. SCE). The reported oxidation potentials were obtained with a scan speed of 100 $mV\,s^{-1}$ unless otherwise indicated. Oxidation of neutral oligomers in solution was accomplished by adding solutions of thianthrenium perchlorate ($THIClO_4$)[41] or nitrosonium tetrafluoroborate ($NOBF_4$) from a gas-tight syringe. UV/Vis/NIR spectra were recorded by using a Perkin Elmer Lambda 900 spectrophotometer equipped with an Oxford Optistat cryostat for variable-temperature experiments. The temperature was kept constant within ±0.3 K, and spectra were corrected for volume changes. The concentrations in the optical experiments varied between 10^{-5} and 10^{-3} M, using both 10 mm and 1 mm near-IR grade suprasil quartz cells. Fluorescence measurements were performed by using a LS50B Perkin Elmer Fluorescence spectrometer. ESR experiments were carried out with an X-band Bruker ESP 300E spectrometer, operating with a high sensitivity cavity, an ER 035 M NMR gauss meter, and a HP 5350B frequency counter.

^1H and ^{13}C NMR spectra of the compounds were recorded in either $CDCl_3$ or $[D_2]$1,1,2,2-tetrachloroethane ($[D_2]$TCE) depending upon their solubility. The ^1H and ^{13}C NMR spectra recorded in $[D_2]$TCE were calibrated with respect to peaks at $\delta=6.0$ and 74.0 (295 K, 300 MHz), respectively. The mass of the compounds was determined by GC-MS and MALDI-TOF-MS techniques. For GC-MS analysis, a small amount of the substance (≈1 mg) was dissolved in $CHCl_3$ (1 mL), injected, and detected at 340 °C by using the initial column temperature at 150 °C. For MALDI-TOF-MS, the substance (1 mg) was dissolved in 1,2,4-trichlorobenzene and mixed with matrix solution of α-cyano-4-hydroxycinnamic acid in THF for analysis.

Theoretical methodology: Quantum-chemical calculations have been performed on the neutral and cationic forms of EDOT*n* and T*n* oligomers. The ground-state geometries of all compounds have been optimized at the Hartree–Fock ab initio level by using a 6-31G basis set (note that the restricted open-shell Hartree–Fock (ROHF) approach has been adopted to deal with the singly charged systems).[42] The optimized geometries were used as input for calculations including electron correlations to describe the optical properties of the molecules investigated. The calculations were based on: i) the Hartree–Fock semiempirical intermediate neglect of differential overlap (INDO) method,[43] coupled to a single configuration interaction (SCI) formalism; ii) the Austin Model 1[44] technique with a full configuration interaction treatment on a limited active space. In the INDO/SCI calculations, all single excitations within the π manifold have been taken into account, and the Coulomb repulsion terms were expressed by the Ohno–Klopman potential;[45] in the case of singly charged species, this potential provided excitation energies in closer agreement with experiment than the more conventional Mataga–Nishimoto potential[46] (usually adopted to describe the absorption spectra of neutral molecules). A block (up to 40) of frontier molecular orbitals was considered to generate an initial set of electronic configurations in the AM1/FCI approach, out of which the most relevant excitations were selected by using perturbation theory.[47]

Materials: Phenylboronic acid, 2-phenylthiophene, trimethyl borate, $[Pd(PPh_3)_4]$, pinacol, and 2,5-diiodothiophene were purchased from Aldrich chemicals and used without further purification. Compounds **3** and **5** were prepared as described in literature.[48] The compounds 2-bromo-

5-phenylthiophene, 5,5′-diiodo-2,2′-bithiophene, and 5,5″-diiodo-2,2′:5′,2″-terthiophene were synthesized following published procedures.[15] Compound 4,4,5,5-tetramethyl-2-phenyl-[1,3,2]-dioxaborolane (**8**) was prepared from phenylboronic acid and pinacol by following the literature procedure.[49]

2,5-Dibromo-3,4-ethylenedioxythiophene (1): A solution of 3,4-ethylenedioxythiophene (14.2 g, 100 mmol) in dimethylacetamide (DMA; 50 mL) was cooled to 0 °C, blanketed by argon. A solution of *N*-bromosuccinimide (37.4 g, 210 mmol) in DMA (100 mL) was added dropwise, and the temperature was maintained below 10 °C. After addition, the reaction mixture was brought to RT at which temperature it was stirred for another hour. The reaction mixture was then poured into ice water (1 L) and filtered, and the residue was washed with water. After crystallization from ethanol, pure product was obtained as a white crystalline material (21.7 g, 72 % yield): m.p. 99 °C; ^{1}H NMR ($CDCl_3$): $\delta = 4.27$ (s, 4H); ^{13}C NMR ($CDCl_3$): $\delta = 139.8$ (C3,4), 85.5 (C2,5), 64.9 (CH_2).

2,5-Bis(trimethylstannyl)-3,4-ethylenedioxythiophene (2): A solution of 3,4-ethylenedioxythiophene (14.2 g, 100 mmol) in dry THF (70 mL) was cooled to −65 °C, blanketed by argon. *n*BuLi (2.5 M, 80 mL) was slowly added dropwise, and the temperature was constantly kept below −55 °C. After addition the reaction mixture was warmed to −20 °C, after which it was cooled to −60 °C again. At this temperature a solution of trimethyltin chloride (40 g, 201 mmol) in dry THF (50 mL) was slowly added, after which the temperature was allowed to reach RT. After one hour of stirring at RT the solvents were removed, and the residue was extracted with CH_2Cl_2/H_2O. The combined organic fractions were dried and filtered, and the solvent was removed to give the product (33.6 g, 72 % yield). It should be noted that, although slightly contaminated with monostannylated product (2-trimethylstannyl-3,4-ethylenedioxythiophene), this bisstannylated compound was used without further purification. ^{1}H NMR ($CDCl_3$): $\delta = 4.14$ (s, 4H), 0.34 (s, 18H); ^{13}C NMR ($CDCl_3$): $\delta = 148.6$, 115.9, 64.7, −8.7.

5,5′-Bis(trimethylstannyl)-2,2′-bi(3,4-ethylenedioxythiophene) (4): This compound was prepared analogously to compound **2** by applying 2,2′-bi(3,4-ethylenedioxythiophene) (**3**, 6.25 g, 22 mmol) in THF (125 mL), *n*BuLi (2.5 M, 18 mL, 45 mmol), and trimethyltin chloride (8.8 g, 44 mmol) in THF (75 mL). After the extraction procedure, the resulting solid was stirred in methanol, filtered, dried, and stirred with *n*-hexane, and this resulted in **4** (9.6 g, 74 % yield). N.B. Although slightly contaminated with monostannylated product, this bisstannylated compound was used without further purification. ^{1}H NMR ($CDCl_3$): $\delta = 4.32$ (d, 4H), 4.22 (d, 4H), 0.35 (s, 18H).

2-Phenyl-3,4-ethylenedioxythiophene (6): A solution of **5** (28.3 g, 93 mmol), iodobenzene (20.8 g, 102 mmol), and *N*,*N*-dimethylformamide (DMF, 100 mL) was deaerated several times and then handled under argon. $[Pd(PPh_3)_2Cl_2]$ (0.50 g, 0.7 mmol) was added, and the mixture was stirred at 85 °C for one hour. The reaction mixture was then poured into ice water and extracted twice with CH_2Cl_2. The combined organic fractions were washed with water, dried (Na_2SO_4), filtered, and concentrated. The residue was purified by vacuum distillation (b.p. 138–140 °C; 0.05 mmHg) to give pure **6** (12.7 g, 63 % yield). ^{1}H NMR ($CDCl_3$): $\delta = 7.73$ (m, 2H), 7.38 (m, 2H), 7.23 (m, 1H), 6.30 (s, 1H), 4.35 (d, 2H), 4.25 (d, 2H).

2-Bromo-5-phenyl-3,4-ethylenedioxythiophene (7): Bromination of **6** was performed analogously to **1** by using **6** (10.5 g, 48 mmol), DMA (60 mL), and NBS (9.4 g, 53 mmol). After pouring the reaction mixture into ice water and extraction with CH_2Cl_2, the combined organic fractions were filtered over a short SiO_2 column, dried (Na_2SO_4), and concentrated. Subsequent recrystallization from methanol resulted in pure **7** (9.0 g, 63 % yield), m.p. 84–85 °C; ^{1}H NMR ($CDCl_3$): $\delta = 7.65$ (m, 2H), 7.37 (m, 2H), 7.23 (m, 1H), 4.30 (m, 4H).

2,5-Diphenyl-3,4-ethylenedioxythiophene (EDOT1): A solution of phenylboronic acid (4.5 g, 37 mmol) and **1** (5.0 g, 16.7 mmol) in toluene (30 mL) and aqueous Na_2CO_3 (1 M; 30 mL) was deaerated several times and placed under argon. $[Pd(PPh_3)_4]$ (0.5 g, 0.4 mmol) was added, and the mixture was stirred under reflux for 10 h. After this period another portion of catalyst (50 mg) was added, after which the reaction mixture was stirred for another 4 h under reflux. The reaction mixture was then poured into CH_2Cl_2/water and extracted with CH_2Cl_2 several times, and the combined organic fractions were washed with water, dried, and concentrated. The resulting solid was recrystallized from ethanol, and this resulted in pure **EDOT1** (2.9 g, 60 % yield), m.p. 104 °C; ^{1}H NMR ($CDCl_3$): $\delta = 7.75$ (m, 4H), 7.38 (m, 4H), 7.25 (m, 2H), 4.35 (s, 4H); ^{13}C NMR ($CDCl_3$): $\delta = 138.6$, 132.9, 128.6, 126.6, 126.1, 115.4, 64.6; UV/Vis (CH_2Cl_2): $\lambda_{max}(\varepsilon) = 344$ nm; GC-MS: *m*/*z* (%): [M^+] 294.

5,5′-Diphenyl-2,2′-bi(3,4-ethylenedioxythiophene) (EDOT2): A solution of **6** (10.0 g, 46 mmol), TMEDA (*N*,*N*,*N*′,*N*′-tetramethyl 1,2-ethanediamine, 10.6 g, 92 mmol), and dry THF (80 mL) was cooled to −20 °C, under argon. *n*BuLi (2.5 M, 18 mL) was added dropwise, and the temperature was kept below −15 °C. After addition, stirring was continued for another 45 min at −15 °C. The reaction mixture was then added dropwise (over a period of 1 h) to a flask containing [Fe(acac)$_3$] (16.2 g, 46 mmol) dissolved in dry THF (80 mL) at 60 °C. After addition, the resulting reaction mixture was stirred for another 3 h under reflux. It was then brought to RT, and the precipitate was filtered, stirred in methanol, filtered again, recrystallized from DMA, filtered, and finally dried. This resulted in pure **EDOT2** (3.7 g, 35 % yield), m.p. 305 °C; ^{1}H NMR ($CDCl_3$): $\delta = 7.72$ (m, 4H), 7.35 (m, 4H), 7.19 (m, 2H), 4.42–4.35 (m, 8H); ^{13}C NMR ($CDCl_3$): $\delta = 137.9$, 137.6, 133.2, 128.6, 126.3, 125.9, 115.3, 108.3, 64.9, 64.8; UV/Vis (CH_2Cl_2): $\lambda_{max}(\varepsilon) = 398$, 416 nm; GC-MS: *m*/*z* (%): [M^+] 434.

5,5″-Diphenyl-2,2′:5′,2″-ter(3,4-ethylenedioxythiophene) (EDOT3): Analogously to **6**, a Stille reaction by using **7** (4.45 g, 15 mmol), **2** (3.5 g, 7.5 mmol), dry DMF (20 mL), and $[Pd(PPh_3)_2Cl_2]$ (40 mg) was performed. After 1 h at 80 °C, the reaction mixture was poured into ice water, and the precipitate was filtered off. Resolution in CH_2Cl_2, followed by filtration over SiO_2, and removal of the solvent, resulted in a solid. The latter was further purified by column chromatography (SiO_2, hexanes/CH_2Cl_2 (1:1)), and this resulted in pure **EDOT3** as a yellow solid (300 mg), m.p. 300 °C; ^{1}H NMR ($CDCl_3$): $\delta = 7.75$ (m, 4H), 7.37 (m, 4H), 7.19 (m, 2H), 4.42 (m, 8H), 4.38 (m, 4H); UV/Vis (CH_2Cl_2): $\lambda_{max}(\varepsilon) = 436$, 462 nm; MALDI-TOF MS: *m*/*z* (%): [M^+]: 574. N.B. Solubility was too low to measure its ^{13}C NMR spectrum.

5,5‴-Diphenyl-2,2′:5′,2″:5″,2‴-quater(3,4-ethylenedioxythiophene) (EDOT4): Analogously to **6**, a Stille reaction using **7** (1.8 g, 3 mmol), **4** (2.0 g, 6.7 mmol), dry DMF (30 mL), and $[Pd(PPh_3)_2Cl_2]$ (50 mg) was performed. After 2 h at 80 °C, the reaction mixture was cooled to RT, and the precipitate was filtered and dried. Subsequently, it was boiled in toluene (150 mL), filtered, (hot), and dried again. This resulted in a red, almost insoluble solid (1.30 g, 62 % yield). MALDI-TOF MS analysis showed that the product is approximately 80 % pure ($M = 714$) (The contaminants are **Ph-EDOT$_6$-Ph** ($M = 994$) and **Ph-EDOT$_{10}$-Ph** ($M = 1554$), which were the result of organotin–bromo exchange followed by Stille couplings); UV/Vis (CH_2Cl_2): $\lambda_{max}(\varepsilon) = 471$, 501 nm.

2-(5-Phenylthienyl)-4,4,5,5-tetramethyl-1,3,2-dioxaborolane (9): *n*-Butyllithium (5 mL, 1.6 M in *n*-hexane) was placed in a three-necked flask containing dry THF (5 mL) and cooled to −78 °C under dry argon. The compound 2-bromo-5-phenylthiopene (1.2 g, 5 mmol) was dissolved in dry THF (10 mL) and added dropwise for 30 minutes at −78 °C. The mixture was stirred at −78 °C for 3 h, and trimethyl borate (8 mL) was added dropwise, and then the mixture was stirred for 1 h, warmed to room temperature, and poured with crushed ice containing concd HCl (15 mL). The white solid was extracted into CH_2Cl_2, dried over anhydrous Na_2SO_4, and the solvent was evaporated to obtain 5-phenyl-2-thienylboronic acid as a solid. This intermediate was dissolved in dry CH_2Cl_2 (25 mL) and refluxed with pinacol (0.6 g, 5 mmol) for 12 h by using a Dean–Stark trap under dry argon. After the reaction, the organic layer was dried over anhydrous Na_2SO_4, and the solvent was evaporated. The crude product was purified by passing it through a silica gel column with 20 % CH_2Cl_2 in *n*-hexane as a eluent. Compound **9** was obtained as a light blue viscous liquid after removal of the solvent (1.1 g, 77 % yield). ^{1}H NMR ($CDCl_3$): $\delta = 7.66$ (d, 2H), 7.61 (d, 1H), 7.39 (m, 3H), 7.30 (m, 1H), 1.36 (s, 12H); ^{13}C NMR ($CDCl_3$): $\delta = 151.6$, 138.6, 134.5, 129.3, 128.2, 126.5, 124.8, 84.4, 25.1; GC-MS [$M_W = 286$]: *m*/*z* (%): 286 [M^+] (purity = 98.0 %).

2,5-Diphenylthiophene (T1): Compound 2,5-diiodothiophene (0.75 g, 2.2 mmol), **8** (1.8 g, 8.9 mmol), and $[Pd(PPh_3)_4]$ (3 mol %) were dissolved in THF (20 mL) and purged with dry argon for 15 minutes at 25 °C. K_2CO_3 (2.44 g, 17.7 mmol) was dissolved in water (5 mL), degassed, and added to the reaction mixture. The reaction mixture was purged again with dry argon for 30 minutes and allowed to reflux for 18 h under argon, then cooled, and poured into water. The pale yellow solid was filtered by using a Buchner funnel. The solid was washed with a cold methanol/water mixture (50:50

  0947-6539/02/0810-2394 $ 20.00+.50/0 *Chem. Eur. J.* **2002**, *8*, No. 10

(*v*/*v*)), dried, and purified by recrystallizing from hot methanol to give **T1** (0.26 g, 50% yield), m.p. 152–154 °C;[15] ^{1}H NMR ($CDCl_3$): $\delta = 7.65$ (d, 4H), 7.40 (m, 4H), 7.31–7.26 (m, 4H); ^{13}C NMR ($CDCl_3$): $\delta = 143.9$, 134.6, 129.1, 127.7, 125.9, 124.2; GC-MS [$M_W = 236$]: *m*/*z* (%): 236 [M^+] (purity = 99%); UV/Vis ($CHCl_3$): $\lambda_{max}(\varepsilon) = 327$ nm.

5,5′-Diphenyl-2,2′-bithiophene (T2): Compounds 5,5′-diiodo-2,2′-bithiophene (0.42 g, 1.0 mmol), **8** (0.8 g, 4.0 mmol), and [$Pd(PPh_3)_4$] (3 mol%) were dissolved in freshly distilled chlorobenzene (20 mL) and purged with dry argon for 15 minutes at 25 °C. K_2CO_3 (1.1 g, 8.0 mmol) was dissolved in water (5 mL), degassed, and added to the reaction mixture. After purging again with dry argon for 30 min, the mixture was stirred at 100 °C for 18 h under dry argon, then cooled, and poured into excess methanol, filtered, dried, and purified by recrystallizing from hot toluene to give **T2** (0.14 g, 44% yield), m.p. 240–243 °C;[15] ^{1}H NMR ([D_2]TCE): $\delta = 7.64$ (d, 4H), 7.42 (m, 4H), 7.32 (m, 2H), 7.28 (d, 2H), 7.21 (d, 2H); ^{13}C NMR ($CDCl_3$): $\delta =$ 143.1, 136.7, 133.9, 129.2, 127.9, 125.7, 124.8, 124.1; GC-MS [$M_W = 318$]: *m*/*z* (%): 318 [M^+] (purity = 99%); UV/Vis ($CHCl_3$): $\lambda_{max}(\varepsilon) = 374$ nm.

5,5″-Diphenyl-2,2′:5′,2″-terthiophene (T3): Compounds 5,5″-diiodo-2,2′:5′,2″-terthiophene (0.5 g, 1 mmol), **8** (0.8 g, 4 mmol), and [$Pd(PPh_3)_4$] (3 mol%) were reacted by using the procedure described for **T2**. After the reaction, the mixture was cooled to room temperature, filtered, and washed with methanol. **T3** was purified by recrystallization from toluene (0.13 g, 33% yield), m.p. 286–289 °C;[15] ^{1}H NMR ([D_2]TCE): $\delta = 7.64$ (d, 4H), 7.42 (m, 4H), 7.32 (m, 2H), 7.28 (d, 2H), 7.21 (d, 2H), 7.15 (s, 2H); ^{13}C NMR ($CDCl_3$): $\delta = 129.2$, 127.9, 125.7, 124.9, 124.6, 124.1; GC-MS: [$M_W = 400$]: *m*/*z* (%): 400 [M^+] (purity = 99%); UV/Vis ($CHCl_3$): $\lambda_{max}(\varepsilon) = 404$ nm.

5,5‴-Diphenyl-2,2′:5′,2″:5″,2‴-quaterthiophene (T4): Compounds 5,5-diiodo-2,2′-bithiophene (0.39 g, 0.93 mmol), **9** (0.8 g, 2.8 mmol), and [$Pd(PPh_3)_4$] (3 mol%) were dissolved in 1,2,4-trichlorobenzene (10 mL) and purged with dry argon for 30 min. K_2CO_3 (0.77 g, 5.6 mmol) was dissolved in water (3 mL), degassed, and added to the reaction mixture. After purging with dry argon for 30 min, the mixture was stirred at 100 °C under dry argon for 18 h, then cooled, filtered, and washed successively with water, methanol, acetone, and CH_2Cl_2. The red solid was purified by recrystallizing from hot 1,2,4-trichlorobenzene, and this yielded **T4** (0.1 g, 22% yield), m.p. 324–328 °C;[15] MALDI-TOF [$M_W = 482$]: *m*/*z* (%): 482 [M^+]; UV/Vis ($CHCl_3$): $\lambda_{max}(\varepsilon) = 425$ nm. An analytically pure sample was obtained by using thermal gradient sublimation. Solubility was too low to measure ^{1}H and ^{13}C NMR data.

Acknowledgements

This work is financially supported by the Dutch Ministry of Economic Affairs, the Ministry of Education, Culture and Science, and the Ministry of Housing, Spatial Planning and the Environment through the E.E.T. program (EETK97115), and by the Council for Chemical Sciences of the Netherlands Organization for Scientific Research (CW-NWO) and the Eindhoven University of Technology in the PIONIER program (98400), and the Institute for the Promotion of Innovation by Science and Technology in Flanders (IWT). The work in Mons is partly supported by the Belgian Federal Government "Interuniversity Attraction Pole in Supramolecular Chemistry and Catalysis (PAI4/11)" and the Belgian National Fund for Scientific Research (FNRS/FRFC). D.B. and R.L. are research associates of the FNRS. The work at the University of Arizona is supported in part by the National Science Foundation (CHE-0078819).

[1] For a recent review article on PEDOT, see: L. Groenendaal, F. Jonas, D. Freitag, H. Pielartzik, J. R. Reynolds, *Adv. Mater.* **2000**, *12*, 481.
[2] a) F. Jonas, L. Schrader, *Synth. Met.* **1991**, *41–43*, 831; b) G. Heywang, F. Jonas, *Adv. Mater.* **1992**, *4*, 116; c) I. Winter, C. Reece, J. Hormes, G. Heywang, F. Jonas, *Chem. Phys.* **1995**, *194*, 207.
[3] M. Dietrich, J. Heinze, G. Heywang, F. Jonas, *J. Electroanal. Chem.* **1994**, *369*, 87.
[4] L. Groenendaal, G. Zotti, F. Jonas, *Synth. Met.* **2001**, *118*, 105.
[5] For more information on AGFA's PEDT/PSS (ORGACON) products, see http://sfc.agfa.com.
[6] a) S. Akoudad, J. Roncali, *Chem. Commun.* **1998**, 2081; b) S. Akoudad, J. Roncali, *Synth. Met.* **1999**, *101*, 149.
[7] D. J. Irvin, C. J. DuBois, J. R. Reynolds, *Chem. Commun.* **1999**, 2121.
[8] L. Huchet, S. Akoudad, E. Levillain, A. Emge, P. Bäuerle, J. Roncali, *J. Phys. Chem.* **1998**, *102*, 7776.
[9] S. Akoudad, P. Frère, N. Mercier, J. Roncali, *J. Org. Chem.* **1999**, *64*, 4267.
[10] K. Müllen, G. Wegner, *Electronic Materials: The Oligomer Approach*, Wiley, Chichester, **1998**
[11] G. A. Sotzing, J. R. Reynolds, P. J. Steel, *Adv. Mater.* **1997**, *9*, 795.
[12] G. A. Sotzing, J. R. Reynolds, P. J. Steel, *Chem. Mater.* **1996**, *8*, 882.
[13] a) G. A. Sotzing, J. R. Reynolds, *J. Chem. Soc. Chem. Commun.* **1995**, 703; b) J. L. Reddinger, G. A. Sotzing, J. R. Reynolds, *Chem. Commun.* **1996**, 1777; c) G. A. Sotzing, J. L. Reddinger, J. R. Reynolds, *Synth. Met.* **1997**, *84*, 199; d) G. A. Sotzing, J. L. Reddinger, A. R. Katritzky, J. Soloducho, R. Musgrave, J. R. Reynolds, *Chem. Mater.* **1997**, *9*, 1578; e) F. Larmat, J. R. Reynolds, B. A. Reinhardt, L. L. Brott, S. J. Clarson, *J. Polym. Sci. Part A: Polym. Chem.* **1997**, *35*, 3627; f) D. J. Irvin, J. R. Reynolds, *Polym. Adv. Technol.* **1998**, *9*, 260; g) J. A. Irvin, J. R. Reynolds, *Polymer* **1998**, *39*, 2339; h) S. A. Sapp, G. A. Sotzing, J. R. Reynolds, *Chem. Mater.* **1998**, *10*, 2101; i) D. J. Irvin, P. J. Steel, D. S. Dudis, J. R. Reynolds, *Synth. Met.* **1999**, *101*, 392; j) J. A. Irvin, F. Piroux, M. C. Morvant, V. L. Robertshaw, A. Angerhofer, J. R. Reynolds, *Synth. Met.* **1999**, *102*, 965; k) B. Tsuie, J. L. Reddinger, G. A. Sotzing, J. Soloducho, A. R. Katritzky, J. R. Reynolds, *J. Mater. Chem.* **1999**, *23*, 299.
[14] R. G. Hicks, M. B. Nodwell, *J. Am. Chem. Soc.* **2000**, *122*, 6746.
[15] S. Hotta, S. A. Lee, T. Tamaki, *J. Heterocycl. Chem.* **2000**, *37*, 25.
[16] S. A. Lee, S. Hotta, F. Nakanishi, *J. Phys. Chem. A* **2000**, *104*, 1827.
[17] a) S. Akoudad, C. Thobie-Gautier, E. Elandaloussi, P. Frère, *J. Chem. Soc. Chem. Commun.* **1994**, 2249; b) P. Blanchard, H. Brisset, B. Illien, A. Riou, J. Roncali, *J. Org. Chem.* **1997**, *62*, 2401.
[18] J. Cornil, D. Beljonne, C. M. Heller, I. H. Campbell, B. K. Laurich, D. L. Smith, J. L. Brédas, *Chem. Phys. Lett.* **1997**, *278*, 139.
[19] a) M. G. Hill, K. R. Mann, L. L. Miller, J.-F. Penneau, *J. Am. Chem. Soc.* **1992**, *114*, 2728; b) M. G. Hill, J.-F. Penneau, B. Zinger, K. R. Mann, L. L. Miller, *Chem. Mater.* **1992**, *4*, 1106; c) Y. Yu, E. Gunic, B. Zinger, L. L. Miller, *J. Am. Chem. Soc.* **1996**, *118*, 1013.
[20] a) P. Bäuerle, U. Segelbacher, A. Maier, M. Mehring, *J. Am. Chem. Soc.* **1993**, *115*, 10217; b) P. Bäuerle, U. Segelbacher, K.-U. Gaudl, D. Huttenlocher, M. Mehring, *Angew. Chem.* **1993**, *105*, 125; *Angew. Chem. Int. Ed. Engl.* **1993**, *32*, 76; c) U. Segelbacher, N. S. Sariciftci, A. Grupp, P. Bäuerle, M. Mehring, *Synth. Met.* **1993**, *55–57*, 4728.
[21] a) G. Zotti, G. Schiavon, A. Berlin, G. Pagani, *Chem. Mater.* **1993**, *5*, 430; b) G. Zotti, G. Schiavon, A. Berlin, G. Pagani, *Chem. Mater.* **1993**, *5*, 620.
[22] a) P. Audebert, P. Hapiot, J.-M. Pernaut, P. Garcia, *J. Electroanal. Chem.* **1993**, *361*, 283; b) P. Hapiot, P. Audebert, K. Monnier, J.-M. Pernaut, P. Garcia, *Chem. Mater.* **1994**, *6*, 1549; c) P. Audebert, P. Hapiot, *Synth. Met.* **1993**, *75*, 95.
[23] a) J. A. E. H. Van Haare, L. Groenendaal, E. E. Havinga, R. A. J. Janssen, E. W. Meijer, *Angew. Chem.* **1996**, *108*, 969; *Angew. Chem. Int. Ed. Engl.* **1996**, *35*, 638; b) J. A. E. H. Van Haare, M. Van Boxtel, R. A. J. Janssen, *Chem. Mater.* **1998**, *10*, 1166.
[24] a) J. P. Prakka, J. A. Jeevarajan, A. S. Jeevarajan, L. D. Kispert, M. P. Cava, *Adv. Mater.* **1996**, *8*, 54; b) J. A. E. H. Van Haare, L. Groenendaal, E. E. Havinga, E. W. Meijer, R. A. J. Janssen, *Synth. Met.* **1997**, *85*, 1091.
[25] A. Sakamoto, Y. Furukawa, M. Tasumi, *J. Phys. Chem. B* **1997**, *101*, 1726.
[26] E. Levillain, J. Roncali, *J. Am. Chem. Soc.* **1999**, *121*, 8760.
[27] J. J. Apperloo, J.-M. Raimundo, P. Frère, J. Roncali, R. A. J. Janssen, *Chem. Eur. J.* **2000**, *6*, 1698.
[28] J. B. Torrance, B. A. Scott, B. Welber, F. B. Kaufman, P. E. Seiden, *Phys. Rev. B* **1979**, *19*, 730, and references therein.
[29] a) D. D. Graf, R. G. Duan, J. P. Campbell, L. L. Miller, K. R. Mann, *J. Am. Chem. Soc.* **1997**, *119*, 5888; b) D. D. Graf, J. P. Campbell, L. L. Miller, K. R. Mann, *J. Am. Chem. Soc.* **1996**, *118*, 5480.
[30] A. Merz, J. Kronberger, L. Dunsch, A. Neudeck, A. Petr, L. Parkanyi, *Angew. Chem.* **1999**, *111*, 1533; *Angew. Chem. Int. Ed.* **1999**, *38*, 1442.
[31] J. J. Apperloo, R. A. J. Janssen, *Synth. Met.* **1999**, *101*, 373.
[32] A. Smie, J. Heinze, *Angew. Chem.* **1997**, *109*, 375; *Angew. Chem. Int. Ed. Engl.* **1997**, *36*, 363.

[33] a) P. Tschuncky, J. Heinze, A. Smie, G. Engelmann, G. Koßmehl, *J. Electroanal. Chem.* **1997**, *433*, 223; b) J. Heinze, H. John, M. Dietrich, P. Tschuncky, *Synth. Met.* **2001**, *119*, 49; c) J. Heinze, C. Willmann, P. Baüerle, *Angew. Chem.* **2001**, *113*, 2936; *Angew. Chem. Int. Ed.* **2001**, *40*, 2861.
[34] J. Cornil, D. Beljonne, J. L. Brédas, *J. Chem. Phys.* **1995**, *103*, 842.
[35] J. L. Brédas, G. B. Street, *Acc. Chem. Res.* **1985**, *18*, 309.
[36] In chemical terminology a *positive polaron* (which is an expression used in solid-state physics) corresponds to a *cation radical*, associated with a local geometry relaxation, see reference [35].
[37] D. Beljonne, J. Cornil, H. Sirringhaus, P. J. Brown, M. Shkunov, R. H. Friend, J. L. Brédas, *Adv. Funct. Mater.* **2001**, *11*, 229.
[38] D. Beljonne, J. Cornil, J. L. Brédas, P. Millié, R. Silbey, *J. Chem. Phys.* **2000**, *112*, 4749.
[39] A. Dkhissi, unpublished results.
[40] J. J. Apperloo, J. A. E. H. Van Haare, R. A. J. Janssen, *Synth. Met.* **1999**, *101*, 417.
[41] H. J. Shine, C. F. Dais, R. Small, *J. Org. Chem.* **1964**, *29*, 21.
[42] Gaussian 98 (Revision A.3), M. J. Frisch, G. W. Trucks, H. B. Schlegel, G. E. Scuseria, M. A. Robb, J. R. Cheeseman, V. G. Zakrzewski, J. A. Montgomery, R. E. Stratmann, J. C. Burant, S. Dapprich, J. M. Millam, A. D. Daniels, K. N. Kudin, M. C. Strain, O. Farkas, J. Tomasi, V. Barone, M. Cossi, R. Cammi, B. Mennucci, C. Pomelli, C. Adamo, S. Clifford, J. Ochterski, G. A. Petersson, P. Y. Ayala, Q. Cui, K. Morokuma, D. K. Malick, A. D. Rabuck, K. Raghavachari, J. B. Foresman, J. Cioslowski, J. V. Ortiz, B. B. Stefanov, G. Liu, A. Liashenko, P. Piskorz, I. Komaromi, R. Gomperts, R. L. Martin, D. J. Fox, T. Keith, M. A. Al-Laham, C. Y. Peng, A. Nanayakkara, C. Gonzalez, M. Challacombe, P. M. W. Gill, B. G. Johnson, W. Chen, M. W. Wong, J. L. Andres, M. Head-Gordon, E. S. Replogle, J. A. Pople, Gaussian Inc., Pittsburg, PA, **1998**.
[43] J. Ridley, M. C. Zerner, *Theor. Chim. Acta* **1973**, *32*, 111.
[44] M. J. S. Dewar, E. G. Zoebisch, E. F. Healy, J. J. P. Stewart, *J. Am. Chem. Soc.* **1985**, *107*, 3702.
[45] a) K. Ohno, *Theoret. Chim. Acta* **1964**, *2*, 219; b) G. Klopman, *J. Am. Chem. Soc.* **1964**, *86*, 4550.
[46] N. Mataga, K. Nishimoto, *Z. Phys. Chem.* **1957**, *13*, 140.
[47] AMPAC 6.0, 1997 Semichem, 7204 Mullen, Shawnee, KS 66216.
[48] S. S. Zhu, T. M. Swager, *J. Am. Chem. Soc.* **1997**, *119*, 12568.
[49] R. A. Bowie, O. C. Musgrave, *J. Chem. Soc.* **1963**, 3945.

Received: October 30, 2001 [F3645]

  0947-6539/02/0810-2396 $ 20.00+.50/0